SSRG International Journal of Electrical and Electronics Engineering
ISSN: 2348-8379/ https://doi.org/10.14445/23488379/IJEEE-V10I1P112

Volume 10 Issue 1, 128-137, January 2023

Original Article

Design of Low Power Ni-chrome-Platinum Micro-Heater for MEMS-Based Gas Sensor in UAV Applications

V. Vinoth Kumar[1], G. Sasikala[2]

[1, 2]*Department of Electronics and Communication Engineering, Vel Tech Rangarajan Dr. Sagunthala R&D Institute of Science and Technology, Chennai, Tamilnadu, India.*

[1]*Corresponding Author : icevinoth@gmail.com*

Received: 02 December 2022 Revised: 09 January 2023 Accepted: 19 January 2023 Published: 29 January 2023

Abstract *- Environmental hazardous gas detection sensors play a major function in various applications. Most of the commercial sensors available in the market with good electrical characteristics; however, these sensors were not suitable for the applications of air quality monitoring using micro-UAV due to power constraints. To our knowledge, the proposed nichrome/platinum-based micro heater provides a better low power consumption of about 6.5 mW for the operating temperature of 812. 62° K and 4mW for the operating temperature of about 381.38° K among the various micro heaters used for MEMS-based gas sensors. The operating temperature of about 80 % can be increased with the same power utilization. Also, the proposed nichrome/platinum-based micro heater design is used to supply uniform heat intensity to the sensor's sensing film to detect high and low concentrations of oxidized gas from the environment. This proposed micro heater platform provides good temperature distribution with low power consumption comparatively with other micro heaters used in MEMS-based gas sensors. Temperature distribution, surface loss density, and power consumption analysis were done for the proposed micro-heater.*

Keywords *- Micro-heater, MEMS gas sensor, Finite Element Method, UAV, Power consumption.*

1. Introduction

Electrical signals generated by the gas sensors due to the reactions with the gas molecules play a vital role in various applications such as biomedical applications for the detection of various gases from the breath, hazardous gas monitoring in industrial areas, air quality monitoring using uncrewed aerial vehicles and several wireless applications. The sensors were designed using 2-D materials and nano technologies to provide high sensitivity and good selectivity for suitable applications [1-6]. High accuracy, less power consumption, improved selectivity, good sensitivity, flexibility, linearity and fast recovery time are required for the gas sensors used in these applications [1,5,7]. Commercially available air quality sensors were used to measure the various environmental pollutants, and the blynk app was used to monitor the parameters [9].

In recent days, low-power gas sensors using metal oxide semiconductors have created more attentiveness comparatively with electrochemical-based sensors [10] and optical-based sensors [11] and less production cost with considerable performance [2]. The major parts of MOS-based gas sensors are micro heater, sensing film and electrodes. Whenever the gas molecules interact with sensing layers at a particular temperature, the electrode senses the change in electrical signal occurring in sensing materials. The external sources give the required power supply for the adsorption or reduction of the gas [12, 13]. However, external power sources like optical and hot chucks are uncomfortable for compact applications. Hence the researchers concentrated more on the micro heaters embedded with sensors and other materials sensitive to measured gases at room temperature [14-28]. Researchers focused more on the materials responsive to room temperature [29-36]. Thus the room temperature responsive sensing materials are synthesised to get nanostructured materials like nanowires and nanoparticles etc., and researchers also focused on embellishing nobel materials like gold, silver, and platinum materials for MEMS-based gas sensor applications [29-36]. Less power consumption was observed from the sensing devices being more responsive at room temperature compared with other sensors with internal heating sources [30-36]; anyway, the room temperature responsive sensors are reactive with atmospheric humidity. However, those effects on the sensor response are difficult to overcome [29, 32]. The heat source required for the MEMS sensors can be established in two different methods: using a micro heater inside the sensor, which is referred to as self-heated MEMS sensor [24-28], and another method is to use a heat source externally to supply the heat to the sensing layer of the sensor [14-22]. The various semiconductor materials

used for designing and fabricating MEMS-based air quality sensors were discussed, and the author compared the characteristics of the sensors from a UAV application point of view [22]. The microheater-implemented sensors exhibited optimized power consumption to sense the nominal gas concentration level. However, a high power requirement is needed for the gas sensor to be sensitive to low concentrations of gases. The author identified that the 35 μW of power consumption by self-heater nanowire sensor senses NO_2 gas at 150° C [26]. Kim et al. [28] observed that the power of 8.3 μW consumed by Au-based nano wire CO sensor at 103° C. However, the self-heat source-based sensors have some limitations in other characteristics of sensors, such as stability and reliability, which are required for gas sensing applications. Sometimes stability issues were observed in the temperature, leading to the change in electrical parameters from the sensor during gas measurement [27].

2. Methodology

Gas sensors fabricated using MEMS technology provide several advantages, such as being more compact, less power consumption, high accuracy, and improved sensitivity and selectivity. The microheater is one of the layers for the MEMS gas sensor and provides an equal intensity of temperature to the next sensor layer. The design of the micro heater provides better performance of the sensor. Vinoth Kumar V et al. [37] used the IoT platform to monitor the various photo voltaic cell parameters, which can be used to monitor the power specification from the ground station, and the system can be used for monitoring the different hazardous gas molecules available in the surrounding using MEMS-based gas sensor.

Dong Geon Jung et al. [38] used the rectangular, meander and mesh pattern geometry for micro-heater design to detect H_2S gas molecules, and the author identified that the power consumed by the sensor was comparatively less for the detection of 0 to 10 ppm of H2S gas concentration with improved sensor characteristics.

Jonam Cho et al. [39] used thin film type of micro-heaters using stretchable elastomer for smart sensor applications. The author obtained some of the better values for detecting 300 ppm of carbon monoxide gas concentration with the micro heater generated a temperature of 102° C.

Tin-Jen Hsueh et al. [40] proposed a ZnO nano wire-based MEMS sensor using Indium-Tin-Oxide as a micro-heater. The author has good sensitivity characteristics for NO gas compared with the presence of other gases.

Jun-gu Kang et al. [41] proposed the micro heater temperature control using a platinum thin film temperature sensor for CO gas measurement. The author observed that the temperature produced by the micro-heater varies linearly with the platinum thin film sensor's electrical resistance and enhanced temperature measurement accuracy.

Nandhini G. Iyer et al. [42] proposed a novel micro-heater design for the sensing layer of the sensor in order to detect the ozone molecules present in the environment. The authors identified that the meander type geometry and spiral type provide enhanced thermal distribution to the next layer of the sensor. The author obtained better temperature equality to the sensing layer for the single meander geometry of the micro-heater.

Jianwen sun et al. [43] proposed the NO_2 gas sensor with a platinum material-based micro–heater. The author observed a better sensitivity for the detection of NO_2 gas, about 100 ppb at around 300°C and the author observed that the platinum micro-heater for NO_2 gas sensor provides optimized power consumption with a recovery time of 58 sec.

Gyuweon Junget al. [44] proposed the NO_2 gas sensor based on MEMS technology. The author used an embedded poly-silicon heating layer to distribute a good intensity of thermal energy to the next portion of the sensing device based on a transducer using transistor technology. The author observed the optimized power consumption of about 1.63 mW at 300°C provided by the micro-heater to sense the low concentration of NO_2 gas.

Abdulla S. Alamiei et al. [45] proposed a poly MUMPs-based sensor with an integrated heating element. The characterization of the heating element was analysed. The author identified that the heating element provides the optimized power consumption with different values of temperature from 25° C to 110° C range and the sensing characteristics of MEMS based sensor varies with the variation of resistance at different temperature provided by the heater element to the sensing layer of the sensor.

Jin-woo park et al. [46] used embedded poly-silicon as a heating element for a transistor-based gas sensor, and the author observed that the power consumed by the heating element increased by 58% by increasing the heater resistance of the material by 12% and also the micro-heater offers the good reliability characteristics to the sensor.

Vishal balasubramanian et al. [47] proposed a 500 μm length of window-type poly silicon micro-heater using the finite element method. The author observed the uniform temperature distribution around 1130.39° K with optimised power consumption and improved sensor sensing and selection characteristics.

J.Lee et al. [48] proposed an electrochemical type CO_2 gas sensor using thin film technology and screen printing

technology. The author observed the optimized power consumption of about 59 mW from a two-semi circled micro-heater, providing an improved temperature distribution to the next portion of the sensing device.

2.1. Proposed Micro-heater

The heating element is one of the essential layers of the micro gas sensor to provide the required temperature intensity to the next portion of the sensor to detect the target gas from the environment. There are two types of micro-heaters proposed in this article. The first novel micro-heating element is for the MEMS-based gas sensor for detecting high CO gas concentration. Another novel micro-heating element is proposed for applying MEMS-based gas sensors for low CO gas concentration. These micro-heaters are designed using Finite Element Method (FEM). The combination of nicrome and platinum materials is used to get the enhanced electro-thermal characteristics for suitable applications.

2.1.1. Nichrome-platinum Micro Heater for High-Temperature Generation

The Materials and Nichrome offer better electrical properties; therefore, the composite materials are used for high-temperature generation.

Fig. 1 shows the novel optimized geometry of the micro-heater proposed for generating high temperatures to the sensing layer sense CO gas molecules. The measurement of the micro-heater is 1.5 mm x 2.0 mm, and the various characteristics of the micro-heater are analyzed using the finite element method. A combination of nichrome and platinum is used for the proposed micro-heater design. Thus, the optimized geometry of the proposed nichrome and platinum micro-heater provides the micro-heater's enhanced electrical and thermal characteristics.

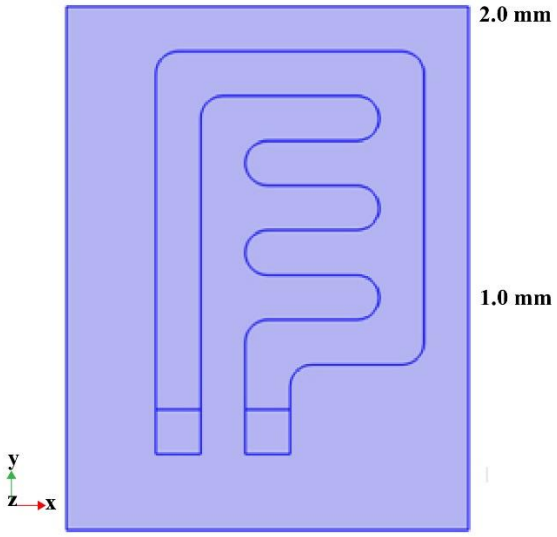

Fig. 1 Geometry and Heat transfer

Table 1. Components of micro heater for high temperature

Specification	Value	Description
Vin	1.5 V	Input voltage
T_layer	10 μm	Layer thickness
Ag Conductivity	6.3 x 10^7 S/m	Electric conductivity of silver
NiCr Conductivity	9.3x5 S/m	Electric conductivity of nichrome
Pt Conductivity	9.43x10^6 S/m	Electric conductivity of platinum
T_Air	20 °C	Air temperature
H_Air	5 [W/(m^2 K)]	Heat transfer film coefficient, air

The silver material is used in both ends of the micro-heater, and a 1.5 V input voltage (V_{in}) is given at one end of the micro-heater. The layer thickness of the micro-heater was chosen as 10 μm. Silver material is used to provide good electrical conductivity to the layer of the micro-heater. The electrical conductivity of nichrome and platinum is 9.3 x 10^5 S/m and 9.43 x 10^6 S/m, respectively. Also, the composition of nichrome and platinum provides a great electro-thermal characteristic required for the micro-heater. In the finite element method, the air temperature was chosen as 28°C with a heat transfer coefficient of 5W/(m^2K). Table 1 shows the parameters of the designed micro-heater.

The finite element method results show the proposed system's temperature distribution analysis. Fig. 2 shows the equal thermal energy supply to the active area of the micro-heating element.

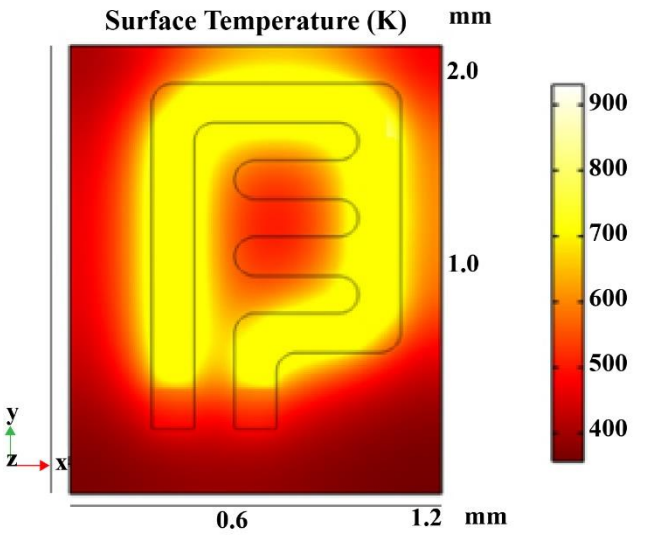

Fig. 2 Temperature distribution Analysis of NiCr/Pt micro-heater for high-concentration CO gas detection

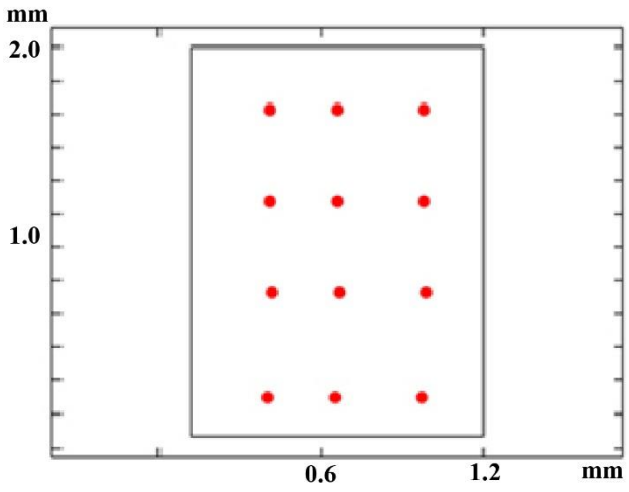

Fig. 3 Temperature distributions analysis of NiCr/Pt micro-heater in active and in-active parts for high-concentration CO gas detection

The point evaluation analyses the thermal energy supply generated by the micro-heating element. NiCr/Pt micro-heater provides high-temperature distribution through the active area of the material due to its optimized geometry and the good electrical characteristics of chosen materials. Fig. 3 shows the point evaluation for temperature distribution throughout the Nicr/Pt micro-heater. It is observed that the temperature is equally distributed to the micro-heater. The temperature point evaluation provides information about the temperature's intensity at various micro-heater points. There are nine different points taken for the analysis purpose, of which six points are taken from the heat-generated area of the heating element, and the remaining three points are taken from the remaining parts of the micro-heater.

Table 2. Temperature distribution of micro heater for high-temperature generation

Points at the active area (mm)	Temperature (°K)
Point:(0.41, 0.72)	810.34
Point:(0.65, 0.72)	813.21
Point:(1.02, 0.72)	812.62
Point:(0.41, 1.42)	810.85
Point:(0.65, 1.42)	811.28
Point:(1.02, 1.42)	810.27
Point:(0.41, 1.67)	812.16
Point:(0.65, 1.67)	811.45
Point:(1.02, 1.67)	811.35
Point:(0.41, 0.72)	352.34
Point: (0.18, 0.72)	351.12
Point: (1.18, 0.72)	352.73

In the active area point of view, nine reference points were taken to analyse the thermal energy distribution of the micro-heating element; it was observed that the maximum temperature of about 812.62 K at the point (1.02, 0.72) and also the temperature around 812.62° K was observed at the remaining eight points of the micro-heater. Temperatures, on the other hand, this temperature is about in the span of 546° C to 552° C, which is suitable for the detection of higher concentrations of CO gas by MEMS-based gas sensors. Similarly, the micro-heating element's in-active area and the micro-heating element's temperatures were observed around 350° K. Table 2. Shows the temperature point evaluation of NiCr/Pt micro-heater for the high concentration of CO gas detection.

2.1.2. Surface Loss Density of Micro-Heater for High-Temperature Application

The surface loss density is one of the important parameters for the design of a micro-heater.

Fig. 4 shows the surface loss density analysis for the high concentration of CO gas detection application. From the result, it is observed that the range of the surface loss density varies from 0.5x104 mW/m to 3.5x104 mW/m. Thus the observed surface loss density, in turn, provides the power consumption of the micro-heater.

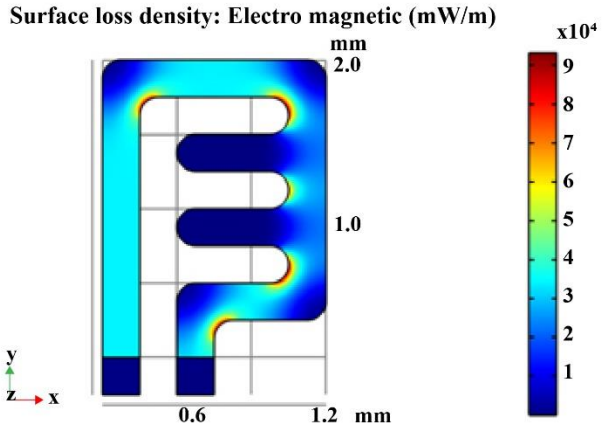

Fig. 4 Surface loss density analysis of NiCr/Pt micro-heater for the high concentration of CO gas detection

2.2. Nichrome-platinum Micro Heater for Low-Temperature Generation

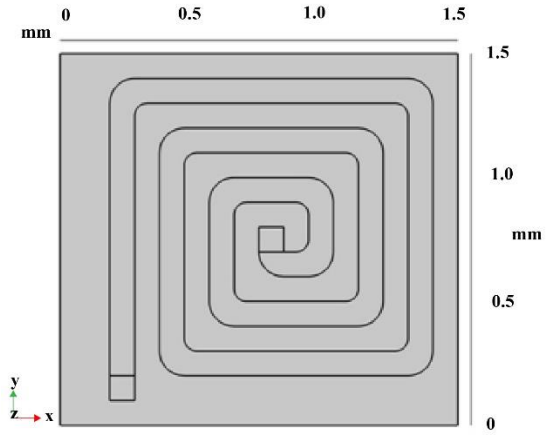

Fig. 5 Geometry of NiCr/Pt micro-heater for low-concentration CO gas detection

Fig. 5 shows the geometry of the spiral-type NiCr/Pt micro-heating element. The measurement of the micro-heating element is 1.5x1.5 mm. The various parameters of the heating element are analysed using the finite element method. Thus, the optimized geometry of the proposed NiCr/Pt micro-heater provides the micro-heating element's enhanced electrical and thermal characteristics.

The silver material is used at both ends of the micro-heating element, and 1.2 V of input voltage (V_in) is given at one end of the heating element. Another end of the heating element is grounded. The layer thickness of the micro-heater is chosen as 10 µm. The silver layer is used to give good electrical conductivity to the micro-heater.

The electrical conductivity of platinum and nichrome is $9.43x10^6$ S/m and $9.3x10^{5,}$ respectively. The simulation results provide the parameters related to the micro-heater's electro-thermal characteristics. Those parameters give information about temperature distribution on the active area of the heating element and surface loss density. The observed parameters of the micro-heater are suitable for the small amount of CO gas.

In the finite element method, the air temperature was chosen as 28°C with a heat transfer coefficient of $5W/(m^2K)$. The point temperature evaluation is done to analyse the temperature distribution around the active area of the micro-heating element. The optimized geometry of the micro-heating element provides the nominal temperature on the micro-heating element's active area, which is suitable for gas sensing applications.

The finite element method results show the proposed system's temperature distribution analysis. Fig. 6 shows almost equal thermal energy to the active area of the NiCr/Pt micro-heating element.

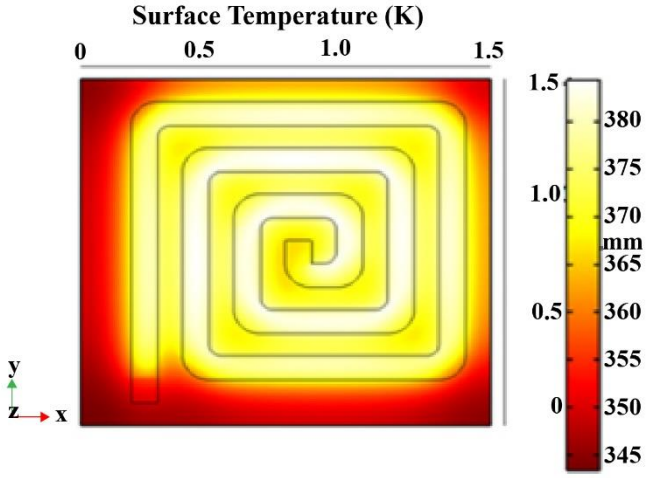

Fig. 6 Temperature distribution Analysis of NiCr/Pt micro-heater for low concentration CO gas detection.

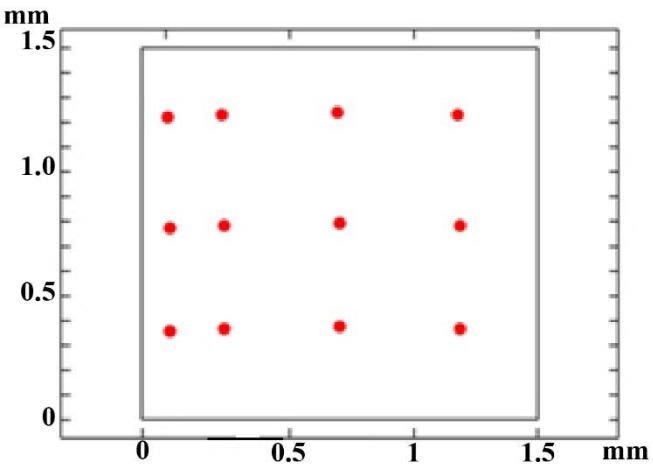

Fig. 7 Temperature distributions analysis of Ni-Cr/Poly silicon micro-heater in active and in-active parts for low concentration of CO gas detection

Fig. 7 shows the point evaluation of temperature distribution on NiCr/Pt micro-heater. It is identified that there is an equal temperature distribution in the active area of the heating element. Thus the point evaluation method for temperature distribution on the micro heater is an efficient method to analyse the thermal energy distribution on the heat generated area. For the remaining parts of the micro-heating element in which, six different points are taken into consideration from the active area, and the remaining three points are taken from the in-active area of the NiCr/Pt micro-heater.

Table 3. Temperature distribution of micro heater for low-temperature generation

Points at the active area (mm)	Temperature (° K)
Point: (0.32, 0.48)	380.41
Point: (0.68, 0.48)	380.75
Point: (1.23, 0.48)	381.26
Point: (0.32, 0.80)	380.32
Point: (0.68, 0.80)	380.63
Point: (1.23, 0.80)	381.38
Point: (0.32, 1.25)	380.21
Point: (0.68, 1.25)	380.47
Point: (1.23, 1.25)	381.13
Point: (0.15, 0.48)	347.23
Point: (0.15, 0.80)	347.10
Point: (0.15, 1.25)	348.42

In the active area point of view, nine reference points were taken to analyse the temperature intensity at various points of the heating element; it was observed that the maximum temperature was about 381.38 K at the point (1.23, 0.80) and also the temperature around 381.38° K was observed at the remaining eight points of the micro-heater.

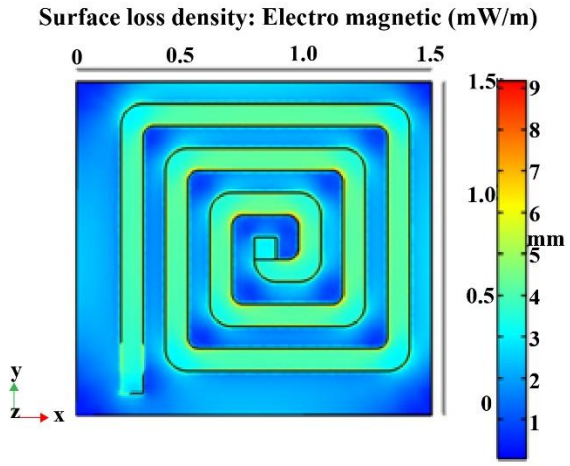

Fig. 8 Surface loss density analysis of NiCr/Pt micro-heater for low-concentration CO gas detection

Temperatures on the other hand, this temperature is about in the range of 107°C to 108° C, which is suitable for the detection of lower concentrations of CO gas by MEMS-based gas sensors. Similarly, from the inactive area of the micro-heater, the temperatures of the micro-heater were observed to be around 348° K. Table 2. Shows the temperature point evaluation of NiCr/Pt micro-heater for low concentration of CO gas detection.

2.2.1. Surface Loss Density Analysis of Micro-Heater for Low-Temperature Application

The surface loss density of the micro-heater is also analyzed for the micro-heater, which provides the nominal temperature generation.

Fig. 8 shows the surface loss density analysis of the NiCr/Pt micro-heater for the small amount of CO gas detection for MEMS gas sensor application. It is observed that around 4 mW/m to 5 mW/m, surface loss density is present in the micro-heater.

3. Result and Discussion

The finite element method is used to analyse the characteristics of the proposed NiCr/Pt microheaters. It is observed that the micro-heater for high-temperature generation and low-temperature generation are more suitable for MEMS-based gas sensors used to detect high and low-concentration CO gas efficiently.

3.1. Analysis of Nichrome-Platinum Micro-Heater for High-Temperature Generation

The various characteristics of NiCr/Pt micro-heater are analyzed for high-temperature generation, such as the temperature variation for the increase in applied voltage, variation of temperature in micro heater with respect to time, heater layer displacement due to thermal reaction and power consumption of the micro-heater.

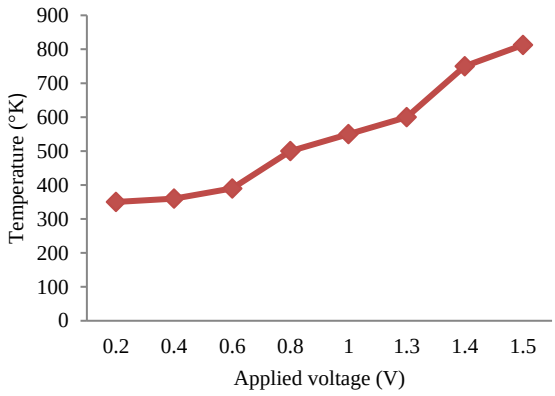

Fig. 9 Applied voltage vs Temperature curve

Thus the thermal energy variation of the micro-heating element for the various magnitude of the applied voltage was analysed using the finite element method. The maximum temperature of about 813.21 ° K was observed for the applied input voltage of about 1.5 V. The temperature of the micro-heating element gradually increased with the applied voltage to the micro-heating element. Fig. 9 shows the relation between the applied voltage and temperature. Thus the maximum temperature generated in the micro-heater can be used to supply equal thermal energy to the next portion of the sensor to sense the high intensity of CO gas molecules.

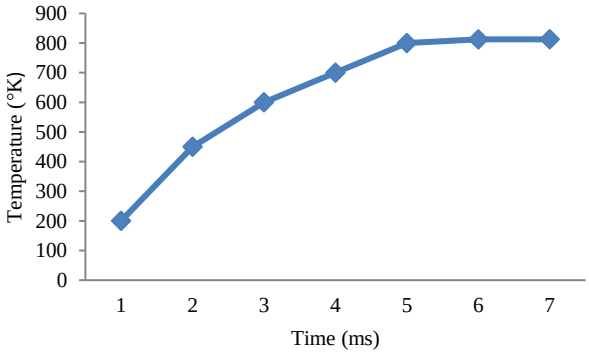

Fig. 10 Time vs Temperature curve

Thus the temperature variation of the micro-heater for the maximum time was analysed using the finite element method. The maximum temperature was about 813.21 ° K was observed for the maximum time duration of around 6.5 ms. The temperature of the micro-heating element gradually increased for the time span of 1 ms to 6.5 ms. Fig. 10 shows the relation between time and temperature. It was observed that the micro heater's maximum temperature reached 6.5 ms. This minimum time duration provides a better response time for the sensor.

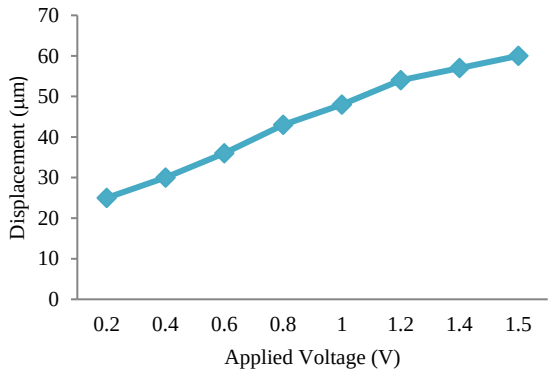

Fig. 11 Applied voltage vs displacement curve

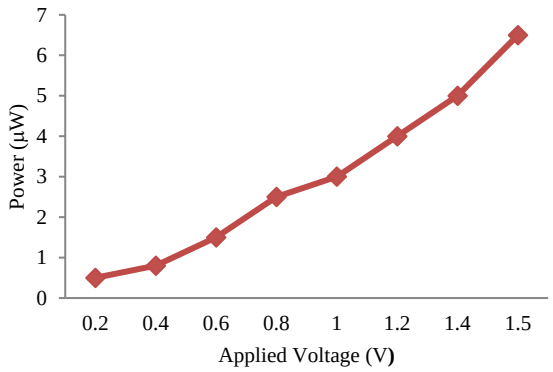

Fig. 12 Applied voltage vs power curve

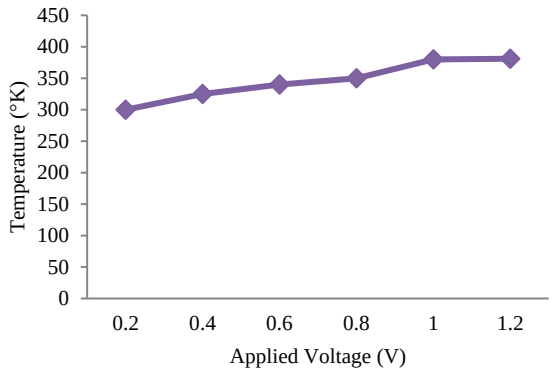

Fig. 13 Applied voltage vs temperature curve

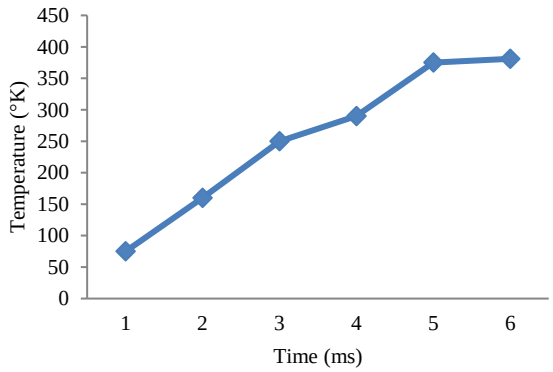

Fig. 14 Time vs Temperature curve

Thus the displacement of the micro-heater surface for the maximum applied voltage was analysed using the finite element method. The maximum displacement of the layer was about 60 µm observed for the maximum applied input voltage of 1.5 V. The displacement of the micro-heater gradually increased for the applied voltage from 0.2 V to 1.5 V. Fig. 11 shows the relation between the applied input voltage and displacement. It was identified that the maximum displacement of the microheater layer was 60 µm. This optimised displacement of the micro-heating element increases the efficiency of the sensing device.

Thus the power consumption of the micro-heating element for the various magnitude of the applied voltage was analysed using the finite element method. The maximum power consumption of 6.5 mW was observed for the input voltage of 1.5 V. The consumed power of the micro-heating element gradually increased with the applied voltage. Fig. 12 shows the relation between the micro-heater's applied voltage and power consumption. Thus the power consumption of the micro-heater to generate high temperature was reduced by using the optimised geometry of the nicrome/platinum micro-heater. This minimum power consumption of the micro-heating element can be used to minimise the overall power consumption of the MEMS sensor.

3.2 Analysis of Nichrome-Platinum Micro-Heater for Low-Temperature Generation

The various characteristics of NiCr/Pt micro-heater are analyzed for low-temperature generation, such as the temperature variation for the increase in applied voltage, variation of temperature in micro heater with respect to time, heater layer displacement due to thermal reaction and power consumption of the micro-heater.

Thus the thermal energy variation of the micro-heating element for the various magnitude of the applied voltage was analysed using the finite element method. The maximum temperature of about 381.38 ° K was observed for the input voltage of 1.2 V. The temperature of the micro-heater gradually increased with the input applied voltage to the micro-heating element. Fig. 13 shows the relation between the applied voltage and temperature. Thus, the maximum temperature generated in the micro-heater can be used to provide a uniform thermal energy supply to the next layer of the sensor to detect a small amount of CO gas.

Thus the temperature variation of the micro-heater for the maximum time was analysed using the finite element method. The maximum temperature was about 381.38 ° K was observed for the maximum time duration of around 6 ms. The temperature of the micro-heating element gradually

increased for the time span of 1 ms to 6 ms. Fig. 14 shows the relation between time and temperature. It was observed that the micro heater's maximum temperature reached 6 ms. This minimum time duration provides a better response time for the sensor.

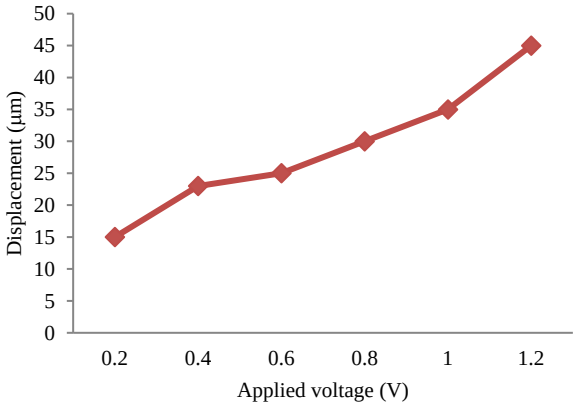

Fig. 15 Applied voltage vs displacement curve

Thus the displacement of the micro-heater surface for the maximum applied voltage was analysed using the finite element method. The maximum displacement of the layer was about 45 µm observed for the maximum applied voltage of 1.2 V. The displacement of the micro-heater gradually increased for the applied voltage from 0.2 V to 1.2 V. Fig. 15 shows the relation between the applied input voltage and displacement. It was observed that the maximum displacement of the microheater layer was 45 µm. This optimised displacement of the micro-heating element increases the efficiency of the sensor.

Thus the consumed power of the micro-heating element for the various magnitude of the applied voltage was analysed using the finite element method. The maximum power consumption of 4 mW was observed for the applied input voltage of 1.2 V. The power consumption of the micro-heater gradually increased with the applied voltage. Fig. 16 shows the relation between the micro-heater's applied voltage and power consumption. Thus the power consumption of the micro-heater to generate high temperature was reduced by using the optimised geometry of the nicrome/platinum micro-heater. This minimum power consumption of the micro-heating element can be used to minimise the overall power consumption of the MEMS sensor.

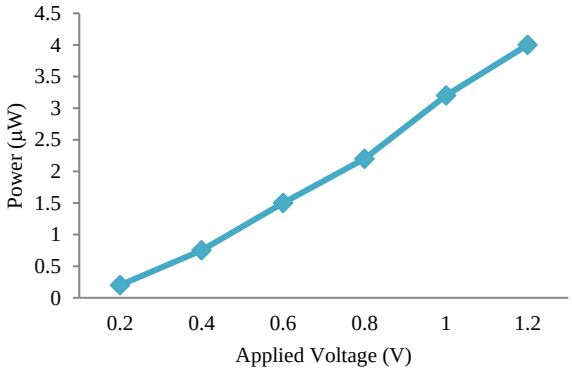

Fig. 16 Applied voltage vs power curve

4. Conclusion

The primary aim of this work is to design a micro-heater for MEMS-based gas sensors. Nowadays, commercially available gas sensors are used for the application of air quality monitoring using UAVs. The power consumed by the UAV air quality sensors is more than the MEMS sensors integrated with UAVs. To increase the endurance of UAVs, it is necessary to reduce the power consumed by MEMS sensors. The low power consumed micro-heating element for the MEMS sensors is designed using the finite element method. Thus the proposed nichrome/platinum micro-heater consumes less power, 6.5 mW for high-temperature generation and 4 mW for a low-temperature generation. The other parameters of the micro heater, such as temperature distribution, surface loss density and displacement with respect to the applied voltage, provide better performance to the MEMS-based CO gas sensor.

References

[1] Winston Yenyu Chen et al., "Nanohybrids of a MXene and Transition Metal Dichalcogenide for Selective Detection of Volatile Organic Compounds," *Nature Communications*, vol. 11, no. 1, p. 1302, 2020. *Crossref*, https://doi.org/10.1038/s41467-020-15092-4

[2] Max M. Shulaker et al., "Three-Dimensional Integration of Nanotechnologies for Computing and Data Storage on a Single Chip," *Nature*, vol. 547, no. 7661, pp. 74-78, 2017. *Crossref*, https://doi.org/10.1038/nature22994

[3] J. van den Broek et al., "Highly Selective Detection of Methanol over Ethanol by a Hand Held Gas Sensor," *Nature Communications*, vol. 10, no. 1, 2019. *Crossref*, https://doi.org/10.1038/s41467-019-12223-4

[4] Shumao Cui et al., "Ultrahigh Sensitivity and Layer-Dependent Sensing Performance of Phosphorene-Based Gas Sensors," *Nature Communications*, vol. 6, no. 1, p. 8632, 2015. *Crossref*, https://doi.org/10.1038/ncomms9632

[5] Radislav A. Potyrailo et al., "Extraordinary Performance of Semiconducting Metal Oxide Gas Sensors Using Dielectric Excitation," *Nature Electronics*, vol. 3, no. 5, pp. 1-10, 2020. *Crossref*, https://doi.org/10.1038/s41928-020-0402-3

[6] Kourosh Kalantar-Zadeh et al., "A Human Pilot Trial of Ingestible Electronic Capsules Capable of Sensing Different Gases in the Gut," *Nature Electronics*, vol. 1, no. 1, pp. 79-87, 2018. *Crossref*, https://doi.org/10.1038/s41928-017-0004-x

[7] Sung H. Lim et al., "An Optoelectronic Nose for the Detection of Toxic Gases," *Nature Chemistry*, vol. 1, no. 7, pp. 562 – 567, 2009. *Crossref*, https://doi.org/10.1038/nchem.360

[8] Radislav A. Potyrailo, "Multivariable Sensors for Ubiquitous Monitoring of Gases in the Era of Internet of Things and Industrial Internet," *Chemical Reviews*, vol. 116, no. 19, pp. 11877–11923, 2016. *Crossref*, https://doi.org/10.1021/acs.chemrev.6b00187

[9] V. Vinoth Kumar, and G. Sasikala, "Internet of Things (IoT) Enabled Air Quality Monitoring System for Conventional and UAV Application," *Nature Environment and Pollution Technology*, vol. 21, no. 1, pp. 71-81, 2022. *Crossref*, https://doi.org/10.46488/NEPT.2022.v21i01.008

[10] Manan Dosi et al., "Ultrasensitive Electrochemical Methane Sensors Based on Solid Polymer Electrolyte-Infused Laser-Induced Grapheme," *ACS Applied Materials & Interfaces*, vol. 11, no. 6, pp. 6166–6173, 2019. *Crossref*, https://doi.org/10.1021/acsami.8b22310

[11] Ayushi Paliwal et al., "Carbon Monoxide (CO) Optical Gas Sensor Based on Zno Thin Films," *Sensors and Actuators B Chemical*, vol. 250, pp. 679 -685, 2017. *Crossref*, https://doi.org/10.1016/j.snb.2017.05.064

[12] Ananya Dey, "Semiconductor Metal Oxide Gas Sensors: A Review," *Materials Science and Engineering B*, vol. 229, pp. 206–217, 2018. *Crossref*, https://doi.org/10.1016/j.mseb.2017.12.036

[13] Z. Q. Zheng et al., "Light-Controlling, Flexible and Transparent Ethanol Gas Sensor Based on Zno Nanoparticles for Wearable Devices," *Scientific Reports*, vol. 5, no. 1, p. 11070, 2015. *Crossref*, https://doi.org/10.1038/srep11070

[14] Incheol Cho et al., "Localized Liquid-Phase Synthesis of Porous Sno2 Nanotubes on MEMS Platform for Low-Power High Performance Gas Sensors," *ACS Applied Materials & Interfaces*, vol. 9, no. 32, pp. 27111-27119, 2017. *Crossref*, https://doi.org/10.1021/acsami.7b04850

[15] Qin Zhou et al., "Fast Response Integrated MEMS Micro Heaters for Ultra Low Power Gas Detection," *Sensors and Actuators A Physical*, no. 223, pp. 67-75, 2015. *Crossref*, https://doi.org/10.1016/j.sna.2014.12.005

[16] Syed Z. Ali et al., "Tungsten-Based SOI Microhotplates for Smart Gas Sensors," *Journal of Micro Electro Mechanical System*, vol. 17, no. 6, pp. 1408 – 1417, 2008. *Crossref*, https://doi.org/10.1109/JMEMS.2008.2007228

[17] Nicodemus M. Sakayo, et al, "Design and Calibration of a Microcontroller Based MQ-4 Gas Sensor for Domestic Cooking Gas System," *SSRG International Journal of Applied Physics*, vol. 6, no. 2, pp. 31-40, 2019. *Crossref*, https://doi.org/10.14445/23500301/IJAP-V6I2P106

[18] Zhengfei Dai et al., "Fast-Response, Sensitivitive and Low-Powered Chemosensors by Fusing Nanostructured Porous Thin Film and Ides-Microheater Chip," *Scientific Reports*, vol. 3, no. 1, p. 1669, 2013. *Crossref*, https://doi.org/10.1038/srep01669

[19] Ameya Rao et al., "In Situ Localized Growth of Ordered Metal Oxide Hollow Sphere Array on Microheater Platform for Sensitive, Ultra-Fast Gas Sensing," *ACS Applied Materials & Interfaces*, vol. 9, no. 3, pp. 2634 – 2641, 2017. *Crossref*, https://doi.org/10.1021/acsami.6b12677

[20] S.E. Moon et al., "A Si FET-type Gas Sensor with Pulse-Driven Localized Micro-Heater for Low Power Consumption," *Sensors and Actuators B Chemical*, vol. 187, pp. 598–603, 2013. *Crossref*, https://doi.org/10.1016/j.snb.2013.05.002

[21] Kwang-Wook Choi et al., "Batch-Fabricated CO Gas Sensor in Large-Area (8-Inch) with Sub-10 Mw Power Operation," *Sensors and Actuators B Chemical*, vol. 289, pp. 153–159, 2019. *Crossref*, https://doi.org/10.1016/j.snb.2019.03.074

[22] Hu Long et al., "In situ Localized Growth of Porous Tin Oxide Films on Low Power Microheater Platform for Low Temperature CO Detection," *ACS Sensors*, vol. 1, no. 4, pp. 339 – 343, 2016. *Crossref*, https://doi.org/10.1021/acssensors.5b00302

[23] Vinoth Kumar V, and Sasikala G, "Strategic Report on MEMS Based Carbon Monoxide Sensor Technology for Environmental Air Quality Monitoring Using Unmanned Aerial Vehicle," *International Journal of Advanced Technology and Engineering Exploration*, vol. 9, no. 93, pp. 1085 – 1110, 2022. *Crossref*, http://dx.doi.org/10.19101/IJATEE.2021.875446

[24] Trinh Minh Ngoc et al., "Ultralow Power Consumption Gas Sensor Based on a Self-Heated Nanojunction of Sno_2 Nanowires," *RSC Advances*, vol. 8, no. 63, pp. 36323–36330, 2018. *Crossref*, https://doi.org/10.1039/C8RA06061D

[25] J. D. Prades et al., "Ultralow Power Consumption Gas Sensors Based on Self-Heated Individual Nanowires," *Applied Physics Letters*, vol. 93, no. 12, p. 123110, 2008. *Crossref*, https://doi.org/10.1063/1.2988265

[26] Nguyen Duc Chinh et al., "Comparative NO_2 Gas-Sensing Performance of the Self-Heated Individual, Multiple and Networked Sno_2 Nanowire Sensors Fabricated by a Simple Process," *Sensors and Actuators B Chemical*, vol. 201, pp. 7–12, 2014. *Crossref*, https://doi.org/10.1016/j.snb.2014.04.095

[27] C.Fàbrega et al., "A Review on Efficient Self-Heating in Nanowire Sensors: Prospects for Very-Low Power Devices," *Sensors and Actuators B Chemical*, vol. 256, pp. 797–811, 2018. *Crossref*, https://doi.org/10.1016/j.snb.2017.10.003

[28] Jae-Hun Kim et al., "Low Power-Consumption CO Gas Sensors Based on Au-Functionalized Sno_2-Zno Core-Shell Nanowires," *Sensors and Actuators B Chemical*, vol. 267, pp. 597–607, 2018. *Crossref*, https://doi.org/10.1016/j.snb.2018.04.079

[29] Daihua Zhang et al., "Detection of NO_2 Down to ppb Levels Using Individual and Multiple In_2O_3 Nanowire Devices," *Nano Letters*, vol. 4, no. 10, pp. 1919 -1924, 2004. *Crossref*, https://doi.org/10.1021/nl0489283

[30] Xia. Y et al., "Confined Formation of Ultrathin ZnO Nanorods/Reduced Graphene Oxide Mesoporous Nanocomposites for High-Performance Room-Temperature NO_2 Sensors," *ACS Applied Materials & Interfaces Nano Letters*, vol. 8, no. 51, pp. 35454 -35463, 2016. *Crossref*, https://doi.org/10.1021/acsami.6b12501

[31] Jun Zhang et al., "Nanostructured Materials for Room-Temperature Gas Sensors," *Advanced Materials*, vol. 28, no. 5, pp. 795–831, 2016. *Crossref*, https://doi.org/10.1002/adma.201503825

[32] Jing Kong et al., "Nanotube Molecular Wires as Chemical Sensors," *Science*, vol. 287, no. 5453, pp. 622–625, 2000. *Crossref*, https://doi.org/10.1126/science.287.5453.622

[33] G. Barillaro, and L.M. Strambini, "An Integrated CMOS Sensing Chip for NO_2 Detection," *Sensors and Actuators B Chemical*, vol. 134, no. 2, pp. 585–590, 2008. *Crossref*, https://doi.org/10.1016/j.snb.2008.05.044

[34] Michela Sainato et al., "Sub-Parts Per Million NO_2 Chemi-Transistor Sensors Based on Composite Porous Silicon/Gold Nanostructures Prepared by Metal-Assisted Etching," *ACS Applied Materials & Interfaces*, Vol. 7, no. 13, pp. 7136-7145, 2015. *Crossref*, https://doi.org/10.1021/am5089633

[35] G. Barillaro, G. M. Lazzerini, and L. M. Strambini, "Modeling of Porous Silicon Junction Field Effect Transistor Gas Sensors: Insight into NO2 Interaction," *Applied Physics Letters*, vol. 96, no. 16, p. 162105, 2010. *Crossref*, https://doi.org/10.1063/1.3391620

[36] G M Lazzerini, L M Strambini, and G Barillaro, "Addressing Reliability and Degradation of Chemi Transistor Sensors by Electrical Tuning of the Sensitivity," *Scientific Reports*, vol. 3, no. 1, pp. 1–8, 2013. *Crossref*, https://doi.org/10.1038/srep01161

[37] Vinoth Kumar, V., and Sasikala, G., "Arduino based Smart Solar Photovoltaic Remote Monitoring System," *Malasian Journal of Science*, vol. 41, no. 3, pp. 58-62, 2022. *Crossref*, https://doi.org/10.22452/mjs.vol41no3.8

[38] Dong Geon Jung et al., "Low-Voltage-Driven SnO_2-Based H_2S Microsensor with Optimized Micro-Heater for Portable Gas Sensor Applications," *Micromachines*, vol. 13, no. 10, p. 1609, 2022. *Crossref*, https://doi.org/10.3390/mi13101609

[39] Jonam Cho, and Gunchul Shin, "Fabrication of a Flexible, Wireless Micro-Heater on Elastomer for Wearable Gas Sensor Applications," *Polymers*, vol. 14, no. 8, p. 1557, 2022. *Crossref*, https://doi.org/10.3390/polym14081557

[40] Ting-Jen Hsueh, Chien-Hua Peng, and Wei-Shou Chen, "A Transparent Zno Nanowire MEMS Gas Sensor Prepared by an ITO Micro-Heater," *Sensors and Actuators B Chemical*, vol. 304, p. 127319, 2020. *Crossref*, https://doi.org/10.1016/j.snb.2019.127319

[41] Kang, Jg., Park, JS., Park, KB. et al. Temperature Control of Micro Heater using Pt Thin Film Temperature Sensor Embedded in Micro Gas Sensor. Micro and Nano Syst Lett 5, vol. 26, 2017. https://doi.org/10.1186/s40486-017-0060-z

[42] Nandini G. Iyer, et al. "Design and Evaluation of Micro-Heater Geometries for MEMS-Based Ozone Gas Sensor through a Theoretical Modeling." *Materials Today: Proceedings*, vol. 66, 2022, pp. 2012-2016, https://doi.org/10.1016/j.matpr.2022.05.446.

[43] Jianwen Sun et al., "Suspended AlGaN/GaN HEMT NO2 Gas Sensor Integrated with Micro-Heater," *Journal of Microelectromechanical Sysetem*, vol. 28, no. 6, pp. 997- 1004, 2019. *Crossref*, https://doi.org/10.1109/JMEMS.2019.2943403

[44] Gyuweon Jung et al., "A Low-Power Embedded Poly-Si Micro-Heater for Gas Sensor Platform Based on a FET Transducer and its Application for NO2 Sensing," *Sensors and Actuators B Chemical*, vol. 334, p. 129642, 2021. *Crossref*, https://doi.org/10.1016/j.snb.2021.129642

[45] Abdullah S. Algamili et al., "Fabrication and Characterization of the Micro-Heater and Temperature Sensor for PolyMUMPs-Based MEMS Gas Sensor," *Micromachines*, vol. 13, no. 4, p. 525, 2022. *Crossref*, https://doi.org/10.3390/mi13040525

[46] Jinwoo Park et al., "Analysis of Cr/Au Contact Reliability in Embedded Poly-Si Micro-Heater for FET-Type Gas Sensor," *Sensors and Actuators B Chemical*, vol. 360, p. 131673, 2022. *Crossref*, https://doi.org/10.1016/j.snb.2022.131673

[47] Vishal Balasubramanian et al., "Electro Thermal Effects of Geometrically Modified MEMS-Based Micro Heater for Gas Sensing Applications," *Sensor Letters*, vol. 17, no. 9, pp. 725 -732, 2019. *Crossref*, https://doi.org/10.1166/sl.2019.4141

[48] J.Lee et al., "Low Power Consumption Solid Electrochemical-Type Micro CO2 Gas Sensor," *Sensors and Actuators B Chemical*, vol. 248, pp. 957–960, 2017. *Crossref*, https://doi.org/10.1016/j.snb.2017.02.040